

Fabrication and characterization of ultra-water-repellent alumina–silica composite films

Takahiro Ishizaki¹, Nagahiro Saito², Yasushi Inoue¹,
Makoto Bekke³ and Osamu Takai¹

¹ EcoTopia Science Institute, Nagoya University, Furo-cho, Chikusa, Nagoya 464-8603, Japan

² Department of Molecular Design and Engineering, Graduate School of Engineering, Nagoya University, Furo-cho, Chikusa, Nagoya 464-8603, Japan

³ Department of Materials Engineering, Graduate School of Engineering, Nagoya University, Furo-cho, Chikusa-ku, Nagoya 464-8603, Japan

E-mail: ishizaki@eco-t.esi.nagoya-u.ac.jp

Received 5 July 2006, in final form 7 November 2006

Published 15 December 2006

Online at stacks.iop.org/JPhysD/40/192

Abstract

Ultra-water-repellent (UWR) films were prepared by microwave plasma-enhanced chemical vapour deposition using trimethylmethoxysilane and aluminium (III) diisopropoxide ethylacetoacetate (ADE) as raw materials. The film was mainly composed of silica and alumina and was apparently transparent. The film thickness was approximately 500 nm. The sample surface was treated with an organosilane in order to introduce hydrophobic groups. The hydrophobic modification led to a water contact angle of more than 150°, whose value corresponds to the UWR surface. The hardness of film with an optimized Al content was significantly improved compared with that without Al. The maximum hardness was 1.71 GPa. In consequence, we successfully prepared an UWR film in the silica–alumina system.

1. Introduction

Ultra-water-repellent (UWR) film has a water contact angle of more than 150°. The water drops on such a surface roll over and over. The characteristic is expected to be applied in various engineering productions such as eyeglasses, lenses and automobile windows [1]. The UWR property is governed by the chemical composition and geometrical structure of surface [2, 3]. A surface becomes more hydrophobic with a lowering of surface energy. As the simplest example, the surface covered with CH₃- or CF₃-groups has low surface energy and water repellent property [4]. However, the surface energy is insufficient to produce UWR films. A suitable roughness or surface texture is required for the UWR films [5–7]. Thus, methods to provide roughness to solid surfaces have been developed [8–17]. Many fabrication methods had been employed to fabricate the UWR surfaces [18–37].

In order to realize the above-mentioned applications, it is necessary for the UWR film to have good mechanical

properties. We have successfully fabricated thin films with ultra-water repellency and high transparency by controlling pressures of organosilane and CO₂ gases in microwave plasma-enhanced chemical vapour deposition (MPECVD) [38]. However, in the previous study, water contact angles of the films were lowered with an increase in the hardness, and the ultra-water repellency was changed into water repellency. This was due to the decrease in surface roughness. We aim to fabricate an UWR thin film with high hardness and high transparency. In order to achieve this aim, we examined a composite material in the silica–alumina system. The alumina component would harden the UWR film without losing the ultra-water repellency and transparency [39–41].

In this research, we report on an UWR film with high hardness and transparency through MPECVD using trimethylmethoxysilane (TMMOS, (CH₃)₃Si(OCH₃)) and (ADE) (C₁₂H₂₃AlO₅) as raw materials. The water repellency and hardness of the films were discussed from the viewpoint of surface nanotextures, sliding angles and alumina content.

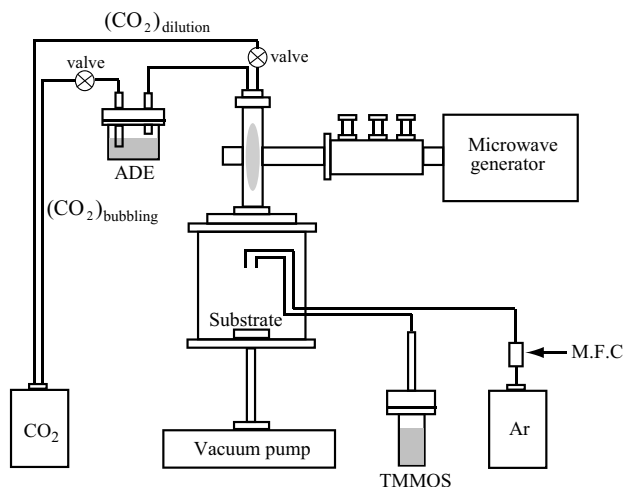


Figure 1. A schematic illustration of the MPECVD apparatus.

2. Experimental procedures

The UWR film was fabricated with a MPECVD system. Figure 1 shows the schematic illustration of the MPECVD system. The MPECVD system consisted of a Vycor glass discharge tube attached with a microwave cavity and a deposition chamber made of stainless steel. The chamber was evacuated down to 6.7 Pa before the deposition. A microwave generator (2.45 GHz) was used at a microwave power of 300 W. The starting materials used were TMMOS, ADE, Ar and CO₂. The partial pressures of TMMOS and Ar were kept constant at 26.7 Pa and 6.7 Pa, respectively. In order to vary the ADE content, the following ratio (R) was adopted:

$$R = \frac{\{P(\text{CO}_2)_{\text{bubbling}} + P(\text{ADE})\}}{\{P(\text{CO}_2)_{\text{dilution}} + P(\text{CO}_2)_{\text{bubbling}} + P(\text{ADE})\}}$$

Here, $P(\text{CO}_2)_{\text{bubbling}}$ was the partial pressure of CO₂ as the bubbling gas, $P(\text{CO}_2)_{\text{dilution}}$ was the partial pressure of CO₂ as the dilution gas and $P(\text{ADE})$ was the partial pressure of ADE. $P(\text{ADE})$ was not obviously independent of $P(\text{CO}_2)_{\text{bubbling}}$. However, $P(\text{ADE})$ would increase while $P(\text{CO}_2)_{\text{bubbling}}$ or R increases. Thus, the ratio, R , is one of the indices related to the ADE content. In this experiment, R was changed from 0 to 1.0, keeping the sum of partial pressure, $P(\text{CO}_2)_{\text{dilution}} + P(\text{CO}_2)_{\text{bubbling}} + P(\text{ADE})$, at 80 Pa. The ADE compound was liquid at room temperature, so we used its vapour after evaporation by introducing CO₂ as the bubbling gas. First, we introduced CO₂ as the bubbling gas, so that the sum of partial pressure, $P(\text{CO}_2)_{\text{bubbling}} + P(\text{ADE})$, could be kept constant. Next, the CO₂ as the dilution gas was introduced, so that the sum of partial pressure, $P(\text{CO}_2)_{\text{dilution}} + P(\text{CO}_2)_{\text{bubbling}} + P(\text{ADE})$, could be 80 Pa. Finally, the total pressure was 113.4 Pa.

The characteristics of the films were mainly controlled by the alumina contents in the film. n-type Si(100) wafers with a size of 2 cm × 2 cm and a thickness of 400 μm or glass plates with a size of 2 cm × 2 cm and a thickness of 1 mm were used as substrates. Before deposition of the UWR films, the substrates were sonically cleaned with ethanol, acetone and ultra-pure water (18.2 MΩ), in that order. The UWR films were then deposited on the cleaned substrates. The substrate

temperature was kept at less than 323 K during the deposition for 15 min. All the film thicknesses were approximately 500 nm. After film deposition, hydrophobic treatment was conducted by the chemical vapour deposition (CVD) method using heptadecafluoro-1,1,2,2-tetrahydro-decyl-1-trimethoxysilane [FAS17; CF₃(CF₂)₇(CH₂)₂Si(OCH₃)₃]. The CVD vessel was sealed with a cap and then heated for 3 h in an electric oven maintained at 423 K. The details were described elsewhere in [42, 43]. All the film thicknesses after this hydrophobic treatment were kept constant at approximately 500 nm, since the molecular film thickness used in hydrophobic treatment was approximately 1–2 nm.

Water contact angles for deposited films were evaluated with a contact angle meter (Kyowa Interface Science, CA-D) based on a sessile drop measuring method with a water droplet 2 mm in diameter. In addition to the water contact angle measurements, the sliding angle measurements were also used as a criterion for the evaluation of super-hydrophobicity of the surface, since the sliding angle is not always low on a surface with a high contact angle. Thus, there has also been an extensive study on the sliding angle behaviour of water droplets [44–47]. Their measurements were conducted in air at 298 K. Hardness of the films was measured by a nanoindenter (Hysitron, TriboScope). A Berkovich-type (three-sided pyramid tip, 142.3°) diamond tip was used as a probe. A force–displacement curve of each sample was obtained under a maximum load of 200 μN. Loading and unloading rates of 40 μN s^{−1} were applied. We estimated the hardness of the films by taking contact areas of the tip/sample into consideration. Our estimation methods for the hardness measurements were based on the method proposed by Oliver and Pharr [48]. The surface morphologies of the UWR films were observed with a field emission scanning electron microscope (FE-SEM; JEOL, JSM-6330F) at an accelerating voltage within the range 5–10 keV. Root mean square roughness (R_{rms}) of the film was acquired in the dynamic force mode with an atomic force microscope (AFM; Seiko Instruments, SPA300HV + SPI-3800N) using a Si probe (Seiko instruments, SI-DF3; force constant: 1.7 N m^{−1}). Chemical bonds in the films were characterized by Fourier transform infrared spectroscopy (FT-IR; Biorad, FTS-175C) and x-ray photoelectron spectroscopy (XPS; Shimadzu-Kratos, AXIS) with MgKα radiation. Absorption spectra were obtained in a transmittance mode. The x-ray source was operated at 12 mA and 20 kV. Optical studies were carried out at room temperature in the transmission mode using a UV/vis spectrophotometer (SHIMADZU UV-1650PC). A glass plate identical to the substrate was used as a reference to determine the total transmission of the UWR layers.

3. Results and discussion

Figure 2 shows the water contact angles on the prepared films as a function of the values of R . All the films prepared had a water contact angle of above 150°, regardless of the value of R . Figures 3(a)–(e) show FE-SEM images of the film surfaces. These images indicate that the value of R had a large effect on their surface morphologies. All the films were composed of fine granular particles. When the value of R was more than 0.5, the films became nondense and the film surfaces had rough

microstructures with pores of approximately 20–100 nm. Most of these particles should be prepared in a clustering process in the gas phase and condensed on the substrate. The clusters led to the irregular surface topography composed of granular particles and nano-scale pores a few hundred nanometres in diameter. Such topography provides ultra-water repellency to the surface [21, 22].

The films deposited at $R = 0$ and 0.25 became denser than those at $R = 0.5, 0.75$ and 1.0. The pore sizes of the films at $R = 0$ and 0.25 were also smaller than those at $R = 0.5, 0.75$ and 1.0. This indicates that the surface roughness of the films at $R = 0$ and 0.25 is more smooth than that at $R = 0.5, 0.75$ and 1.0. However, the film deposited at the lower value of R (<0.5) also had ultra-water repellency. It is known that a water

contact angle of the film surface strongly depends on the types of functional groups on the surface nano-structure [49, 50]. In this study, same hydrophobic treatments were conducted for all samples, so that only surface structure would have an effect on the water contact angle. In order to investigate the effects, root mean square roughnesses (R_{rms}) and water drop sliding angles for all the films were measured. Figure 4 shows the relationships among the water drop sliding angle, the surface roughness (R_{rms}) and the value of R . The water drop sliding angle decreases with the increase in R . On the other hand, the surface roughness increases with the increase in R . This means that the increase in the value of R has a large effect on the surface roughness and the water drop sliding angle has a closer relationship with the surface roughness. The increase in the surface roughness would make the film nondense and form a porous structure in the film. The nondense film would permit an enhancement of the surface air fraction in the pores and reduce the actual area of the rough surface contacted with the water. Therefore, it is considered that the wettability is governed by Cassie–Baxter theory [51] and the sliding angle is lowered.

Figure 5 shows chemical compositions of the films obtained by XPS analysis. All the films mainly consisted of O and Si. With the addition of ADE into the reaction chamber, the film contained a small amount of Al. The Al contents in the films increase slightly with the increase in R . The contents of Si in the film are kept almost constant, while some changes in the O and C contents are observed. The O contents in the film decrease with the increase in the C contents. This relationship can be ascribed to the change in chemical bonding states in the film such as the siloxane network and Al–O bonds. Fourier transform infrared (FT-IR) spectra of the films at given values of R are shown in figure 6.

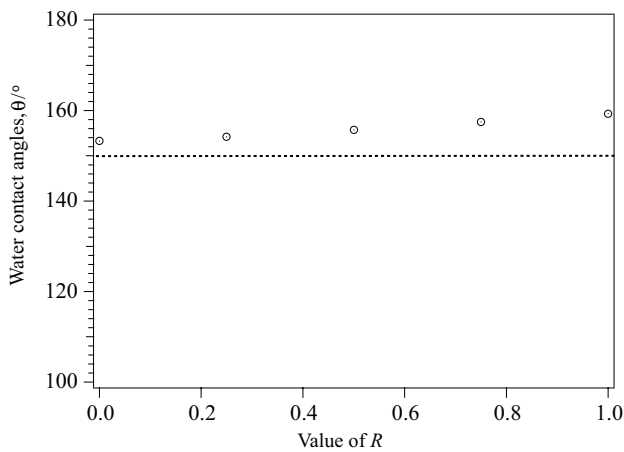


Figure 2. The relationships between water contact angles and the value of R .

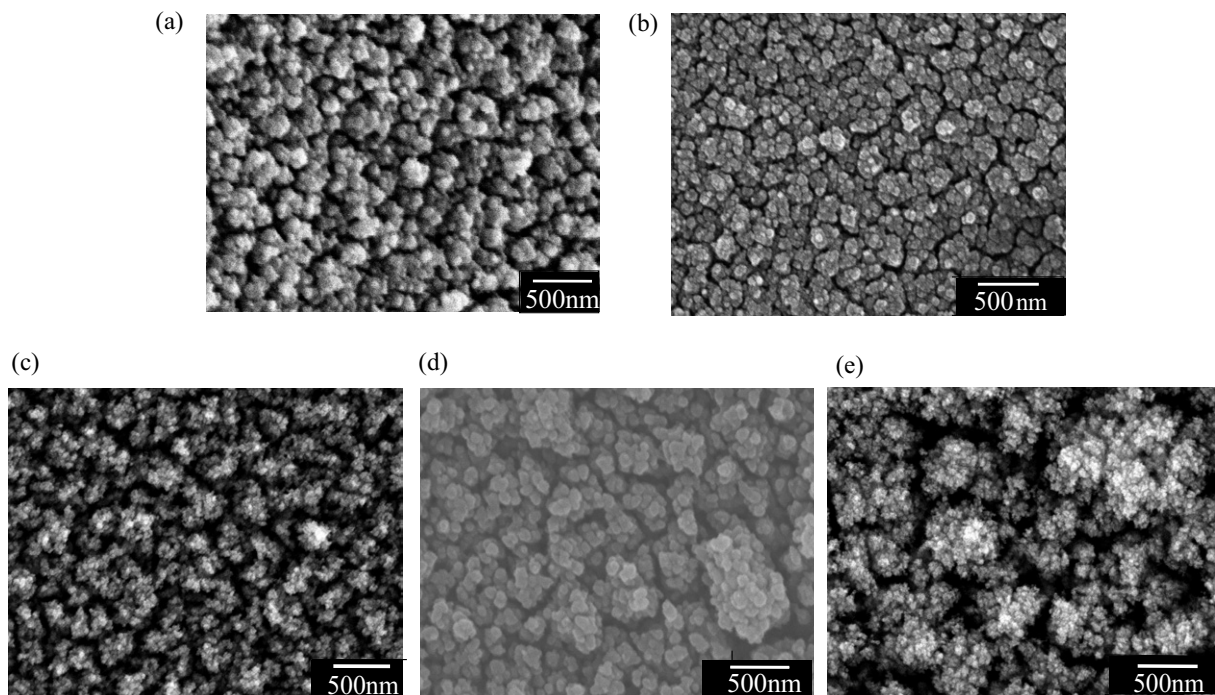


Figure 3. FE-SEM images of nanotextured surfaces deposited by MPECVD with different values of R . (a) $R = 0$, (b) $R = 0.25$, (c) $R = 0.5$, (d) $R = 0.75$ and (e) $R = 1.0$.

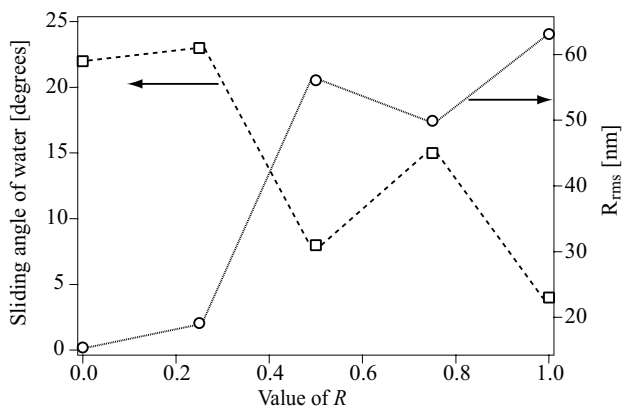


Figure 4. The relationships between sliding angles for water drops, the surface roughness (R_{rms}) and the value of R .

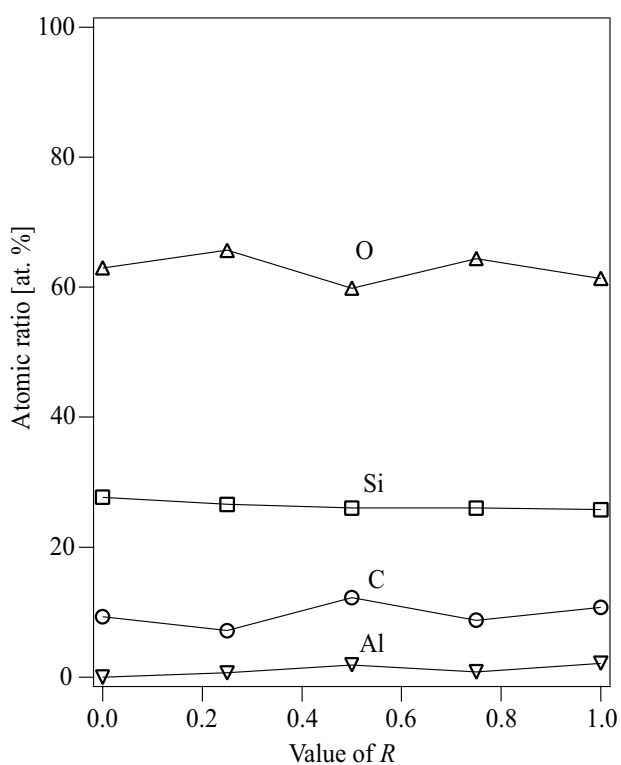
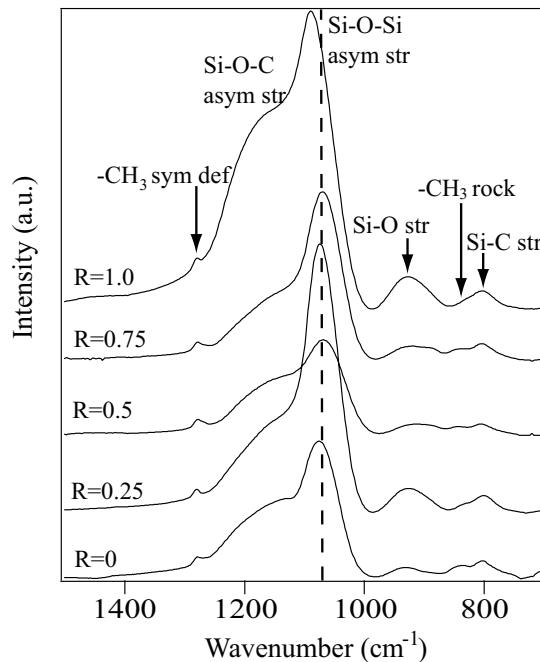


Figure 5. Atomic ratio of the films deposited at various values of R .

In the FT-IR spectra, the peaks at $\sim 814\text{ cm}^{-1}$ and $\sim 1076\text{ cm}^{-1}$ are assigned to the Si-CH₃ stretching and the asymmetric Si-O-Si stretching, respectively. When the value of R was equal to one, the peak originating from the asymmetric Si-O-Si stretching was shifted to a higher wavenumber. FE-SEM images also showed that the particle sizes in the film became bigger. These results indicate that the size of the siloxane network in the film becomes bigger with the increase in R . In addition, the peaks assigned to the asymmetric Si-O-Si stretching mode became broader with the increase in the value of R . The change in the peak position indicates that the bond states in the film changed. The absorption originating from the -CH₃ deformation vibration in Si-CH₃ groups appeared at $\sim 852\text{ cm}^{-1}$ and $\sim 1256\text{ cm}^{-1}$. The absorption assigned to Si-O-CH₃ stretching in the raw material was also observed at



Si-C str	814 cm^{-1}	Si-O-Si asym str	$\sim 1076\text{ cm}^{-1}$
-CH symdef	852 cm^{-1}	Si-O-C asym str	$\sim 1111\text{ cm}^{-1}$
Si-O str	895 cm^{-1}	-CH ₃ sym def in Si-CH ₃	$\sim 1256\text{ cm}^{-1}$

Figure 6. FT-IR spectra of the thin films prepared on the Si substrate with different values of R . (a) $R = 0$, (b) $R = 0.25$, (c) $R = 0.5$, (d) $R = 0.75$ and (e) $R = 1.0$.

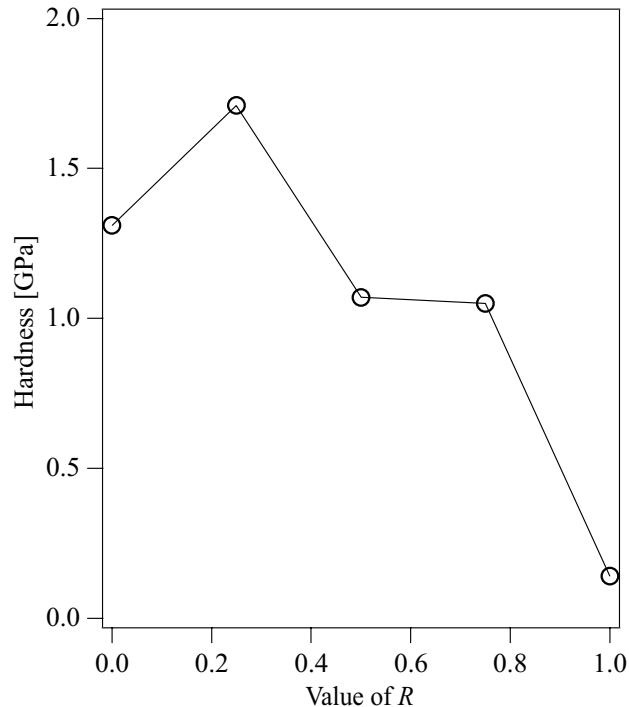


Figure 7. Hardness of the deposited films at various values of R .

$\sim 1111\text{ cm}^{-1}$. The FT-IR analyses provide us information that all the films mainly consisted of SiO_x and -CH₃.

Figure 7 shows the relationship between the hardness of the film and the value of R . The film deposited at R of

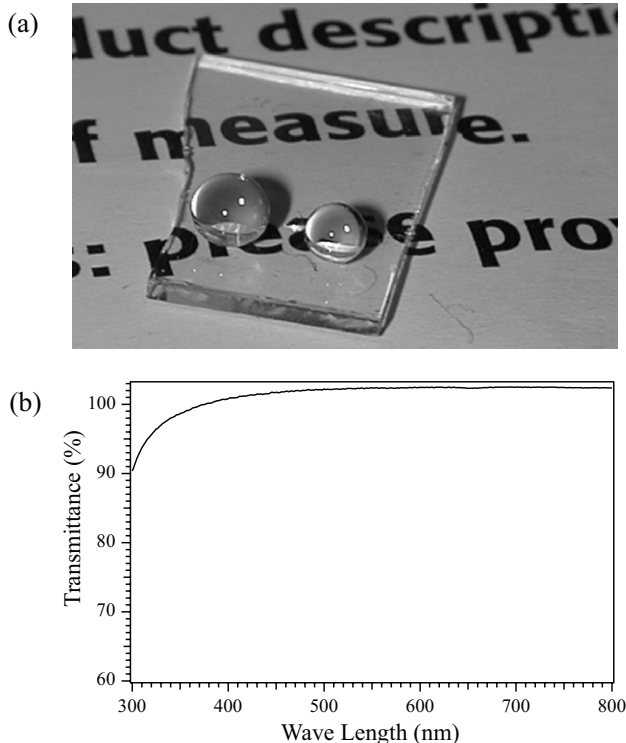


Figure 8. (a) Photograph of water droplets placed on the film prepared on the glass substrate. The film was deposited at the value of R of 0.25. (b) Visible light transmittance of the film prepared at $R = 0.25$.

0.25 had a hardness of 1.71 GPa. This value corresponds to an approximately 30% increase in hardness compared with that of the film composed of only silica. However, the hardness drastically decreases with the increase in R (>0.25). The decrease in hardness may be due to the lowering of the film density originating from the presence of nano-size pores. FT-IR and hardness measurements revealed that the siloxane network structures in the film were closely related to the hardness of the film. As indicated in figure 3, the pore size in the film prepared at $R = 0.25$ was smallest in all the films obtained. As the value of R increased, the film became nondense and the pore size in the film became bigger. The addition of a suitable ADE amount would lead to the formation of a bigger cluster size in the clustering process due to the increase in the siloxane network, resulting in the formation of the dense film. In short, the film would become harder as it becomes denser. This agrees well with the results of the FE-SEM images and hardness measurements.

The UWR film was deposited on the glass substrate to investigate the transparency. The photograph of a water drop on the UWR film prepared at R of 0.25 is shown in figure 8(a). We can clearly read the printed characters under the UWR-coated glass. This indicates that the film on the glass substrate had high optical transparency. Figure 8(b) represents transmittance spectra in the visible range. The film exhibited slightly higher than 100% transmittance due to the suppression of surface reflection. The optical transmittance of the film was more than 90% in the visible range.

4. Conclusions

We successfully fabricated an UWR film with high hardness and high transparency through MPECVD using TMMOS and ADE as raw materials and a hydrophobic treatment using fluoroalkylsilane. The suitable additional amount of ADE leads to a large improvement in the hardness. This improvement corresponds to an approximately 30% increase in hardness compared with that of the film composed of only silica. We believe that the films have wide applications in various manufacturing processes.

Acknowledgments

This work has been supported in part by research project 'Nagoya Nano-Technology Cluster of Innovative Production System' of the Ministry of Education, Culture, Sports, Science and Technology.

References

- [1] Tsujii K, Yamamoto T, Onda T and Shibuichi S 1997 *Angew. Chem. Int. Edn. Engl.* **36** 1011
- [2] Gau H, Herminghaus S, Lenz P and Lipowsky R 1999 *Science* **283** 46
- [3] Hui M and Blunt M J 2000 *J. Phys. Chem. B.* **104** 3833
- [4] Nishino T, Meguro M, Nakamae K, Matsushita M and Ueda Y 1999 *Langmuir* **15** 4321
- [5] Erbil H Y, Demirel A L, Avci Y and Mert O 2003 *Science* **299** 1377
- [6] Liu H, Li S, Zhai J, Li H, Zheng Q, Jiang L and Zhu D 2004 *Angew. Chem. Int. Edn. Engl.* **43** 1146
- [7] Lee W, Jin M-K, Woo W-C and Lee J-K 2004 *Langmuir* **20** 7665
- [8] Sasaki H and Shouji M 1998 *Chem. Lett.* **293** 27
- [9] Murase H, Nakanishi K, Kogure H, Fujibayashi T, Tamura K and Haruta N 1994 *J. Appl. Polym. Sci.* **54** 2051
- [10] Welters W J and Fokkink L G 1998 *Langmuir* **14** 1535
- [11] Dettre R H and Johnson R R Jr 1963 *Adv. Chem. Ser.* **43** 136
- [12] Bartell F E and Shepard J W 1953 *J. Phys. Chem.* **57** 211
- [13] Ogawa N, Soga M, Takada Y and Nakayama I 1993 *Japan. J. Appl. Phys.* **32** L614
- [14] Matsumoto Y and Ishida M 2000 *Sensors Actuators* **83** 179
- [15] Kunigi Y, Nonaku T, Chong Y-B and Watanabe N 1993 *J. Electroanal. Chem.* **353** 209
- [16] Shibuichi S, Yamamoto T, Onda T and Tsujii K 1998 *J. Colloid Interface Sci.* **208** 287
- [17] Bico J, Marzolin C and Quere D 1999 *Europhys. Lett.* **47** 220
- [18] Onda T, Shibuichi S, Satoh N and Tsujii K 1996 *Langmuir* **12** 2125
- [19] Shibuichi S, Onda T, Satoh N and Tsujii K 1996 *J. Phys. Chem.* **100** 19512
- [20] Yamauchi G, Miller J D, Saito H, Takai K, Ueda T, Takazawa H, Yamamoto H and Nishi S 1996 *Colloids Surf.* **116** 125
- [21] Tadanga K, Koriko N and Minami T 1997 *J. Am. Ceram. Soc.* **80** 1040
- [22] Tadanga K, Koriko N and Minami T 1997 *J. Am. Ceram. Soc.* **80** 3213
- [23] Bonnar M P, Burnside B M, Little A, Reuben R L and Wilson J I B 1997 *Chem. Vapor Depos.* **3** 201
- [24] Hozumi A and Takai O 1997 *Thin Solid Films* **303** 222
- [25] Shibuichi S, Yamamoto T, Onad T and Tsujii K 1998 *J. Colloid Interface Sci.* **208** 287
- [26] Hozumi A and Takai O 1998 *Thin Solid Films* **334** 54
- [27] Sasaki H and Shouji M Y 1998 *J. Surf. Finish. Soc. Japan* **49** 944

- [28] Bonnar M P, Burnside B M, Christie J, Sceal E J, Troup C E and Wilson J I B 1999 *Chem. Vapor. Depos.* **5** 1117
- [29] Nakagawa T and Soga M 1999 *J. Non-Cryst. Solids* **260** 167
- [30] Nakajima A, Fujishima A, Hashimoto K and Watanabe T 1999 *Adv. Mater.* **11** 1365
- [31] Hozumi A, Ushiyama K, Sugimura H and Takai O 1999 *Langmuir* **15** 7600
- [32] Rascon C and Parry A O 2000 *Nature* **407** 986
- [33] Miwa M, Nakajima A, Fujishima A, Hashimoto K and Watanabe T 2000 *Langmuir* **16** 5754
- [34] Nakajima A, Hashimoto K and Watanabe T 2000 *Langmuir* **16** 7044
- [35] Öner D and McCarthy T J 2000 *Langmuir* **16** 7777
- [36] Wu Y, Sugimura H, Inoue Y and Takai O 2002 *Chem. Vapor. Depos.* **8** 47
- [37] Teshima K, Sugimura H, Inoue Y, Takai O and Takano A 2004 *Chem. Vapor. Depos.* **10** 295
- [38] Wu Y, Bekke M, Inoue Y, Sugimura H, Kitaguchi H, Liu C and Takai O 2004 *Thin Solid Films* **457** 122
- [39] Liu Y Y, Chen X Q and Xin J H 2006 *Nanotechnology* **17** 3259
- [40] Li J, Fu J, Cong Y, Wu Y, Xue L J and Han Y C 2006 *Appl. Surf. Sci.* **252** 2229
- [41] Kako T, Nakajima A, Kato Z, Uematsu K, Watanabe T and Hashimoto K 2002 *J. Ceram. Soc. Japan.* **110** 186
- [42] Sugimura H, Shiroyama H, Takai O and Nakagiri N 2001 *Appl. Phys. A.* **72** S285
- [43] Saito N, Hayashi K, Sugimura H, Takai O and Nakagiri N 2001 *Chem. Phys. Lett.* **349** 172
- [44] Chen W, Fadeev A Y, Hsieh M C, Öner D, Youngblood J and McCarthy T J 1999 *Langmuir* **15** 3395
- [45] Youngblood J P and McCarthy T J 1999 *Macromolecules* **32** 6800
- [46] Miwa M, Nakajima A, Fujishima A, Hashimoto K and Watanabe T 2000 *Langmuir* **16** 5754
- [47] Schwartz L and Eley R R 1996 *J. Colloid Interface Sci.* **179** 37
- [48] Oliver W C and Pharr G M 1992 *J. Mater. Res.* **7** 1564
- [49] Quere D 2005 *Rep. Prog. Phys.* **68** 2495
- [50] Nakajima A, Hashimoto K and Watanabe T 2001 *Mon. chem.* **132** 31
- [51] Cassie A B D and Baxter S 1944 *Trans. Faraday. Soc.* **40** 11